

AD-A218 745

4

AD

TECHNICAL REPORT ARCCB-TR-90004

DTIC FILE COPY

**FRACTURE TOUGHNESS AND FATIGUE
CRACK INITIATION TESTS OF WELDED
PRECIPITATION-HARDENING STAINLESS STEEL**

J. H. UNDERWOOD

G. P. O'HARA

R. A. FARRARA

J. J. ZALINKA

J. R. SENICK

JANUARY 1990



**US ARMY ARMAMENT RESEARCH,
DEVELOPMENT AND ENGINEERING CENTER
CLOSE COMBAT ARMAMENTS CENTER
BENÉT LABORATORIES
WATERVLIET, N.Y. 12189-4050**



APPROVED FOR PUBLIC RELEASE; DISTRIBUTION UNLIMITED

90 03 05 014

DISCLAIMER

The findings in this report are not to be construed as an official Department of the Army position unless so designated by other authorized documents.

The use of trade name(s) and/or manufacturer(s) does not constitute an official indorsement or approval.

DESTRUCTION NOTICE

For classified documents, follow the procedures in DoD 5200.22-M, Industrial Security Manual, Section II-19 or DoD 5200.1-R, Information Security Program Regulation, Chapter IX.

For unclassified, limited documents, destroy by any method that will prevent disclosure of contents or reconstruction of the document.

For unclassified, unlimited documents, destroy when the report is no longer needed. Do not return it to the originator.

20. ABSTRACT (CONT'D)

stainless steels used for the welds and parent plate of the beam. Three-point bend specimens were used to measure both fatigue crack initiation life and the J-integral fracture toughness of the parent plate and weld-metal in various conditions. The notch fatigue analysis method of Barsom and Rolfe was used to analyze the crack initiation test results. The crack was lengthened, side notches were added, and J_{IC} tests were performed using ASTM Method E-813 with a modified load-line displacement unloading-compliance procedure to measure crack growth.

The following conclusions were drawn: (1) J_{IC} can be accurately determined with a three-point bend test using load-line displacement to measure crack growth by unloading compliance. An accurate expression for a/W in terms of load-line displacement was developed. (2) Fatigue crack initiation life and J_{IC} fracture toughness of stainless steels in various conditions were characterized. The welded and aged condition, with no intermediate solution treatment, showed unstable, cleavage-type fracture and resulted in a low J_{IC} value and a short initiation life.

UNCLASSIFIED

TABLE OF CONTENTS

	<u>Page</u>
ACKNOWLEDGEMENTS	iii
INTRODUCTION	1
METHODS	1
General Procedure	1
Materials	2
Instrumentation	2
Fatigue Crack Initiation	3
J_{Ic} Test Procedures	4
J Calculation	4
Unloading Compliance	5
RESULTS	7
J_{Ic} Fracture Toughness	7
Fatigue Crack Initiation	9
SUMMARY	11
REFERENCES	12

TABLES

I.	SUMMARY OF J_{Ic} AND FATIGUE CRACK INITIATION TESTS PERFORMED WITH STAINLESS STEEL PLATE AND WELD-METAL	13
II.	COMPOSITIONS OF PRECIPITATION-HARDENING STAINLESS STEEL PLATE AND WELD-METAL	14
III.	CALCULATED ELASTIC CRACK-MOUTH-OPENING DISPLACEMENT, v , AND LOAD-LINE DISPLACEMENT, d , FOR A THREE-POINT BEND SPECIMEN	15
IV.	J_{Ic} RESULTS FOR STAINLESS STEEL PLATE AND WELD-METAL IN VARIOUS CONDITIONS	16
V.	CALCULATED STRESS INTENSITY FACTOR, K , FOR STANDARD SINGLE-EDGE CRACK SPECIMEN AND DOUBLE-EDGE CRACK WELD SPECIMEN LOADED IN THREE-POINT BENDING	17

LIST OF ILLUSTRATIONS

1.	Welded box beam configuration showing orientation of test specimen	18
2.	Test specimen for fracture toughness and fatigue crack initiation tests	19
3.	Test equipment for unloading-compliance J_{IC} tests (a) Servo-hydraulic machine control (b) X-Y plotter arrangement	20
4.	Load displacement behavior for 15-500 weld; welded and aged at 593°C	21
5.	J versus crack growth for 95-15 plate; solution treated, aged at 530°C	22
6.	J versus crack growth for 17-400 and 95-14 welds in various conditions	23
7.	Scanning electron microscope fractographs of 17-400 welds; (a) welded, treated, aged (b) welded, aged	24
8.	Fatigue crack initiation behavior of 15-500 and 17-400 welds in various conditions	25
9.	Deformed finite element model of stiffener-to-bottom plate weld specimen	26
10.	Fatigue life described by $[K/r^{1/2} S_y]$ parameter for specimens of different materials and configurations	27

INTRODUCTION

A welded stainless steel structure recently experienced an unanticipated failure while being subjected to fatigue testing by the U.S. Army. In the Spring of 1988 the primary box beam of a proprietary structure, shown schematically in Figure 1, failed in the area of the bottom plate. Excessive deformation of the structure during fatigue loading prompted test personnel to reinspect the bottom plate area where cracks were observed in the vicinity of the welds. Further inspection and investigation revealed that the cracks initiated at notches caused by partial penetration welds of the stiffener plates to the bottom plate. Sharp notches were formed in the gap between the stiffener and the slot in the bottom plate. Cracks initiated at these notches and grew to a length of several centimeters in about 1000 load cycles.

The objective of this report is to describe the fracture toughness and fatigue crack initiation characterization of the type of precipitation-hardening stainless steels used for the welds and parent plate of the structure. This information was required to understand the cause of the failure and implement corrective action. A description of the overall investigation, the cause of failure, and corrective aspects will be given elsewhere. Material characterization tests are the emphasis here. Although analyses of fatigue initiation tests and fracture toughness tests are quite different, a common sample was successfully used for both types of tests. This report describes the tests and results.

METHODS

General Procedure

Three-point bend notched specimens were used to measure both fatigue crack initiation life and J-integral fracture toughness of plate and weld-metal in

various conditions. The nominal specimen configuration shown in Figure 2 was used for plate specimens and specimens made from full penetration weld samples. The materials and conditions tested are shown in Table I, along with representative data to show the general nature of the results; details are discussed later in this report. Fatigue loading was applied to the notched specimen and the number of cycles to crack initiation was determined. The notch fatigue life analysis method of Barsom and Rolfe (ref 1) was used to analyze the test results. The crack was lengthened, side notches were added, and J_{IC} tests were performed using a modified ASTM E-813 procedure (ref 2).

Materials

Five precipitation-hardening stainless steels with 15 percent chromium and 5 percent nickel nominal composition were tested: plate and weld-filler metal designated 95-15 and 95-14, respectively, from which the structure under investigation was fabricated; plate designated 15-5 PH; weld-filler metals 15-500 and 17-400, as specified in AMS 5826 and 5825, respectively. Chemical compositions of these five steels are given in Table II, based on measurements from the current work and prior related work (ref 3) and on specifications in the case of two of the weld-filler metals. The composition measurements in the current work were made with a direct reading emission spectrometer. There was no indication that the composition of the steel was outside of the appropriate specification.

Instrumentation

The fatigue initiation tests were performed on a servo-hydraulic test system in load control. A pragmatic definition of crack initiation was adopted for these tests, that is, the number of cycles required for a surface crack to initiate and grow across the full 3-mm thickness of the notch root. The point of initiation was determined using a low power microscope and also by carefully

noting the change of the displacement range of the test system instrumentation as the fatigue test proceeded.

The J_{IC} tests were run in displacement control using the ramp-type function generator of the test system. A ramp command signal was used to load the specimen to the first level chosen for performing unloading-compliance crack length measurements. The manual set control was then used to partially unload the specimen, and the unloading slope was recorded at ten times the X and Y gains used for the primary recording of load versus displacement. After each unloading was completed, the ramp loading was resumed to continue the test to the next hold and unload position. Figure 3 shows block diagrams of the equipment and signals necessary to perform the loading and recording.

Two highly stable adjustable power supplies were necessary to obtain suitable 10X gain unloading-compliance plots. Two X-Y plotters of the high impedance-type were used, with inputs capable of accepting a floating signal and common mode voltages of about +10 or -10 volts. This was necessary because the 10X gain plotter measured the difference between two voltage signals--that of the load or displacement transducer and that of the power supply output. Polarities were strictly observed in order to obtain only a difference signal.

Fatigue Crack Initiation

The Barsom and Rolfe approach (ref 1) for characterizing fatigue crack initiation has been used for ASTM A723 high strength steels with various notch geometries (ref 4), therefore it was applied to the steels of similar strength level in this investigation. The approach is based on the expression for the maximum notch stress, S_m , normal to the major axis of an elliptical notch with radius r

$$S_m = 1.12 K/(r)^{1/2} \quad (1)$$

where K is the appropriate opening mode stress intensity factor for the notch geometry and applied loading. This relation is exact only as $r \rightarrow 0$, but it provides a useful characterizing of notch root stress and associated fatigue initiation life at notches with a radius of a few millimeters or less (refs 1,4).

The $K/(r)^{1/2}$ approach was used here to compare the measured fatigue lives from the three-point bend specimens of the type shown in Figure 2 with lives from test specimens cut from partial penetration welds in the structure. The only additional information needed was the K solution for the partial penetration weld specimen. This was obtained by finite element analysis, as discussed in the Results section.

J_{IC} Test Procedures

In general, the procedures for performing and analyzing the J_{IC} tests were the ASTM E-813 (ref 2) procedures with one significant modification, that is, the use of a displacement measured on the bottom surface of the specimen and somewhat off the load line. This displacement was used for both J calculations and for unloading-compliance crack length measurements, whereas E-813 requires a load-line displacement for J calculations and a crack-mouth-opening displacement for crack length measurements. If the modified simpler approach using bottom surface displacement were shown to be suitable, it would be a considerable advantage, particularly for small bend specimens. The following sections on J calculation and unloading compliance address the modified procedure.

J Calculation

The use of a modified displacement for J calculation can be considered in relation to Figure 2. The displacement on the bottom surface, d' , was measured near the load line, and was converted to load-line displacement, d , as follows:

$$d = d' (S/2L) \quad (2)$$

Equation (2) would give the same displacement as that measured exactly at the load line if there were ideal rigid body displacements on the bottom surface. Recent analysis (ref 5) showed this to be essentially the case. Elastic finite element results of bottom surface displacements showed, for example, that when $2L/S = 0.9$ and $a/W = 0.6$, the value of displacement calculated from Eq. (2) was within 0.8 percent of the load-line displacement result obtained directly from the finite element analysis. Also, it must be kept in mind that the total load-line displacement in a J_{IC} test is often controlled by plastic deformation in the ligament ahead of the crack. This causes a rigid body-type rotation of the bottom surface, as described by Eq. (2).

The calculation of J included the Eq. (2) expression for d , but otherwise followed the procedures of ASTM Methods E-813 (ref 2) and E-1152 (ref 6). The calculation is outlined as follows:

$$J_i = (P_i S f(a_0/W)/(B B_n)^{1/2} W^{3/2})^2 [(1-\mu^2)]/E + \Sigma_i (|P_i + P_{i-1}| [d(p)_i - d(p)_{i-1}]/b_0 B_n) \quad (3)$$

In Eq. (3) P_i and $d(p)_i$ are the load and the increment of plastic displacement for a given unloading (see Figure 4), a_0 and b_0 are the starting crack length and uncracked ligament, respectively, $f(a_0/W)$ is from the three-point bend K expression of ASTM Method E-399 (ref 7), B_n is net specimen thickness after side notching, and μ and E are Poisson's ratio and elastic modulus, taken as 0.3 and 207,000 MPa, respectively. Equation (3) was used to calculate J except on the two occasions of unstable fracture, one of which is shown in Figure 4. In these cases an average load was calculated and used for P_i , rather than using the load at the point of unloading.

Unloading Compliance

Load-line displacement can be used in place of crack-mouth displacement for measurement of unloading-compliance crack growth, provided that an expression

for a/W in terms of load-line displacement is available. A new expression for a/W in terms of d was developed here, based on the available expression (ref 8) for d in terms of a/W . The new expression is

$$a/W = 1.00051 - 4.15266 U + 9.74768 U^2 - 214.202 U^3 \\ + 1604.31 U^4 - 4633.41 U^5 \quad (4)$$

where

$$U = 1/([dE(B B_n)^{1/2}/P]^{1/2} + 1)$$

for the range

$$0.2 < a/W < 1.0$$

The new inverse expression, Eq. (4), represents the earlier expression (ref 8) with an accuracy of 0.0010 a/W . For a narrower range, $0.40 < a/W < 0.85$, the new expression represents the earlier expression with an accuracy of 0.0002 a/W . Therefore, it is accurate enough for general use in unloading-compliance calculations, including calculations which iterate between the displacement expression and the a/W expression.

Another requirement for the use of load-line displacement in unloading-compliance calculations is that this type of displacement is adequately sensitive to crack length changes in the geometry range of intended use. A comparison of crack-mouth and load-line displacements as a function of crack length is shown in Table III. The dimensionless parameters vEB/P and dEB/P were obtained from References 9 and 8, respectively. Note that for a/W below 0.2, dEB/P has poor sensitivity to a change in a/W and should not be used to measure crack length; vEB/P should be used in this range. For a/W above 0.2, either displacement can be used.

RESULTS

J_{IC} Fracture Toughness

Table IV lists the results of twenty J_{IC} tests for the five materials in various conditions, the effective yield strength, S_y, and the calculated ratio of specimen thickness, B, to the ASTM E-813 thickness requirement for a valid J_{IC} test, 25J/S_y. For a valid-sized sample, the ratio [BS_y/25J] must equal unity or more. Four test results from the prior related work (ref 3) are listed for comparison. The general trend of the tests here is that the available 3-mm nominal material thickness was adequate for a valid result in most cases. Two of the ten pairs of results gave an average ratio of thickness to valid size below unity, that is, 0.54 and 0.82, but all other pairs had one or both values above unity.

The directional nature of J_{IC} for the 95-15 plate is demonstrated in Figure 5. This plot of J versus crack growth data for the T-L and L-T orientations shows that the longitudinal toughness is about three times the transverse value. This significant difference is due to the existence of delta ferrite which is elongated during the hot rolling operation (ref 10). The 95-15 material is a semi-austenitic stainless steel, with an austenitic structure at room temperature after solution treatment. This allows rolling to thin plate or forming to small radii, which are advantages for producing complex structures. A disadvantage of this material is the anisotropy caused by the delta ferrite. Figure 5 also shows good correspondence between the earlier results (ref 3), which used a different lot and thickness of material, and the current results.

A comparison of key J-integral fracture toughness results of the investigation is presented in Figure 6. It shows J versus crack growth results for the 95-14 weld-metal in the condition used in the structure along with a prospective future replacement weld material, 17-400 in three heat treat conditions. The

highest toughness results were from 17-400 conventionally solution treated and aged, followed by 17-400 as-welded, 95-14 conventionally processed, and finally, 17-400 aged-only. This last, lowest toughness result was from specimen 7A-4, the second specimen that displayed unstable fracture in a manner similar to that shown for 15-500 aged-only (see Figure 4). The J versus crack growth curve for the unstable fracture in Figure 6 was not fit with the usual power-law E-813 procedure because of the instability; linear segments were used to connect the unloading data points. However, it is clear from Figure 6 that both J_{IC} and the J-integral toughness following additional crack growth were significantly reduced for the welded and aged 17-400 material. Table IV shows this value and the value for the other unstable fracture to be the lowest toughness observed for the 15-500 and 17-400 materials. It is important to note from Figure 6 that the unstable fracture results in toughness values which are progressively lower than those of the other conditions as crack growth progresses.

Scanning electron microscope fractographs of 17-400 welds in the highest and lowest toughness conditions of Figure 6 are shown in Figure 7. The solution treated and aged sample (Figure 7a) showed classic dimpled rupture, whereas the aged-only sample (7b) showed evidence of cleavage. Visual examination could also distinguish between the two; the solution treated and aged sample had a uniform region of fast fracture, whereas the aged-only sample contained shiny faceted regions on the fast fracture surface. The occurrence of cleavage in the aged-only samples is in agreement with other results (refs 11,12). The as-welded microstructure contains dendrites of ferrite, austenite, and martensite, which when aged directly after welding are susceptible to cleavage. Bosworth and Zvanut (ref 11) found that directly-aged 15-500 and 17-400 welds resulted in lower strength and toughness than solution treated and aged welds.

Fatigue Crack Initiation

Fatigue tests were performed with specimens as shown in Figure 2 for the 15-500 and 17-400 weld materials in three conditions and at four load levels, twenty-four tests in all. The results are shown in Figure 8. A nominal bending stress at the ligament ahead of the notch, S_n , was calculated as follows (see Figure 2 for nomenclature):

$$S_n = 1.5 PS/B(W-a)^2 \quad (5)$$

The number of cycles required for initiation across the full width of the specimen varied by less than a factor of two for the highest nominal stress and by larger amounts at lower stress, as is expected in fatigue. Generally, the aged-only condition for both materials showed the shortest initiation life.

Fatigue crack initiation at partial penetration welds in the structure is believed to have had a major effect on the life of the structure, so it would be useful to compare the initiation life at partial penetration welds to the results from the test specimens of Figure 2. The $K/(r)^{1/2}$ approach (ref 1) can be used for this comparison. For the test specimen in Figure 2, the two basic parameters, K and r , are known. For the partial penetration weld in the structure, a finite element solution is required to calculate K . Figure 9 shows the finite element grid; half of the weld is shown because of the usual symmetry argument. Two notches formed by the gaps between the stiffener plate and the slot in the bottom plate were modeled. The ratio of total width of weld to the plate thickness, t , is 2.91; the ratio of the total plate plus weld thickness, W to t , is 1.27. The penetration of a typical weld into the bottom plate was up to about 50 percent penetration, with a minimum of about 0 percent penetration (that is, no penetration into the thickness of the bottom plate), as shown in Figure 9.

The K results from the finite element model for the double-edge notch with

S/W = 11, corresponding to the tests of partial penetration weld specimens cut from the structure, are shown in Table V. The results are compared with the standard single-edge notched-bend specimen of ASTM Method E-399 (ref 7). Note that the dimensionless K parameter used in Table V includes the specimen span, S; this produces about the same value of the K parameter for quite different values of S/W. Generally, the double notch weld specimen results are about 10 percent higher than those of the standard single notch specimen. We interpret this to be an indication that the reduction in specimen depth, W, away from the center line of the weld causes a significant increase in K for the weld specimen over that of the standard specimen. This increase in K more than makes up for the decrease in K which is expected due to the two cracks.

Fatigue lives from the standard specimen tests are compared directly with lives from weld specimens cut from the structure in Figure 10. The values of K for the r = 1.5-mm tests are from the E-399 relation for the Figure 2 geometry; for the r = 0.13-mm tests, K is from the Table V results and r is defined by the gap between the stiffener and the slot in the bottom plate. Note that the ordinate of Figure 10 includes the effective yield strength to account for the important effect of strength on fatigue initiation life. Including S_y also makes the values dimensionless and thus usable in any set of units. Note also that the data for r = 1.5 mm is initiation life, whereas the data for r = 0.13 mm is total life. This is a reasonable comparison because the total lives for the r = 0.13-mm tests are believed to be predominantly initiation cycles.

The most significant feature of the results in Figure 10 is that the fatigue lives of four materials are well represented by a single expression. The straight line shown, obtained by power-law regression of the r = 1.5-mm data, has the formula

$$N = 85,000[1.12 K/r^{1/2} S_y]^{-5.7} \quad (6)$$

and a correlation coefficient of 0.96. This expression can be used to describe (or predict, for a courageous user) a fatigue initiation life at a notch with a radius of about 2 mm or less, and for which a solution for K is known. The lives for the weld specimens with $r = 0.13$ mm are typically about twice those from Eq. (6), so the equation has some application to the partial penetration welds as well, even though it is somewhat conservative. Of course, higher lives for the $r = 0.13$ -mm specimens are expected, considering that these tests include growth as well as initiation cycles.

SUMMARY

1. J_{IC} test procedures for the three-point bend specimen were developed using a near load-line bottom surface displacement for unloading-compliance measurements of crack growth. A new expression for a/W in terms of load-line displacement was developed.

2. J_{IC} toughness was measured for two plate and three weld-metal precipitation-hardening stainless steels in various welded and heat treated conditions. Measurements were made from samples which were cut from welds, including some samples which displayed cleavage failure due to an incomplete heat treatment following welding.

3. Fatigue crack initiation life was measured for two plate and three weld-metal steels in various conditions. Lives from 1,000 to 1,000,000 cycles were measured using a 1.5-mm radius notch in three-point bend specimens subjected to ligament stresses of about the yield strength level.

4. The ratio of maximum notch-root stress defined by a $K/(r)^{1/2}$ parameter to material yield strength gave a good description of fatigue crack initiation for four steels. The approach also gave an approximate description of initiation for other tests with one of the steels using samples with a significantly different notched configuration.

REFERENCES

1. J.M. Barsom and S.T. Rolfe, Fracture and Fatigue Control in Structures, Prentice-Hall, Englewood Cliffs, NJ, 1987.
2. "Standard Test Method for J_{IC} , A Measure of Fracture Toughness, ASTM E-813," Annual Book of ASTM Standards, Vol. 03.01, American Society for Testing and Materials, Philadelphia, PA, 1989, pp. 698-712.
3. R.A. Farrara, "Fatigue - Fracture Properties of a Semi-Austenitic PH Stainless Steel," Report MRL-R-1041, Materials Research Laboratories, Melbourne, Australia, February 1987.
4. J.H. Underwood, "Fatigue Life Analysis and Tensile Overload Effects with High Strength Steel Notched Specimens," in: High Pressure in Science and Technology, Part II, (C. Homan, R.K. MacCrone, E. Whalley, eds.) Elsevier, New York, 1984, pp. 209-214.
5. J.H. Underwood and M.D. Witherell, "Load-Line Displacements for Three-Point Bend J Tests Using Bottom Surface Displacements," submitted to Engineering Fracture Mechanics.
6. "Standard Test Method for Determining J-R Curves, ASTM E-1152," Annual Book of ASTM Standards, Vol. 03.01, American Society for Testing and Materials, Philadelphia, PA, 1989, pp. 814-824.
7. "Standard Test Method for Plane-Strain Fracture Toughness of Metallic Materials, ASTM E-399," 1989 Annual Book of ASTM Standards, Vol. 03.01, ASTM, 1989, pp. 487-511.
8. J.H. Underwood, J.A. Kapp, and F.I. Baratta, "More on Compliance of the Three-Point Bend Specimen," International Journal of Fracture, Vol. 28, 1985, pp. R41-R45; also, ARDC Memorandum Report ARCCB-MR-85015, Benet Weapons Laboratory, Watervliet, NY, May 1985.
9. H. Tada, P.C. Paris, and G.R. Irwin, The Stress Analysis of Cracks Handbook, Del Research Corp., Hellertown, PA, 1973, p. 2.17.
10. Metals Handbook Ninth Edition, Vol. 9, Metallography and Microstructures, American Society for Metals, 1985, p. 285.
11. T.J. Bosworth and A.J. Zvanut, "Development of a Direct Aging Filler Metal for Welding 15-5 PH/17-4 PH Steel," Welding Research Supplement, June 1977, pp. 159s-170s.
12. H. Schichtmann, "High-Speed Craft Ride on Welded Hydrofoils," Welding Design and Fabrication, March 1981, pp. 91-95.

TABLE I. SUMMARY OF J_{IC} AND FATIGUE CRACK INITIATION TESTS PERFORMED WITH STAINLESS STEEL PLATE AND WELD-METAL

Type	Material	Condition	J_{IC} ; typical KN/m	Initiation; $S_n=1000$ MPa cycles
Plate:	95-15	treat*, age at 530°C: L-T orientation	180	7,000
		T-L orientation	70	- -
	15-5 PH	treat**, age at 593°C	200	17,000
Weld:	95-14	treat*, age at 530°C	80	- -
	15-500	as welded:	120	23,000
		age at 593°C:	80-160	15,000
		treat, age at 593°C:	160	26,000
	17-400	as welded:	100	20,000
age at 593°C:		80-150	14,000	
treat, age at 593°C:		150	22,000	

*Heat treatment of 95-15 and 95-14: solution treat at 1050°C (5 min), air cool; condition at 750°C (2 hrs), air cool; cool to below -5°C (2 hrs); age at 530°C (2 hrs), air cool

**Heat treatment of 15-5 PH: solution treat at 1040°C (1/2 hr), air cool; age at 593°C (4 hrs), air cool

TABLE II. COMPOSITIONS OF PRECIPITATION-HARDENING STAINLESS STEEL PLATE AND WELD-METAL

	Cr	Ni	Mo	Cu	Mn	Si	C	S	P	Nb	Ti
Plate:											
95-15 (measured; ref 3)	15.9	5.5	1.8	1.8	1.33	0.36	0.07	0.007	0.020	0.05	0.09
15-5 PH (measured; current)	15.2	4.4	--	3.1	0.80	0.75	0.04	0.010	0.018	--	--
Weld:											
95-14 (measured; ref 3)	14.2	5.4	1.5	1.8	0.72	0.41	0.04	0.004	0.019	0.24	--
15-500 (AMS 5826)	14.4 15.3	4.8 5.5	0.3 max	3.0 3.5	0.25 0.75	0.60 max	0.025 0.050	0.010 max	0.020 max	-- --	-- --
17-400 (AMS 5825)	16.0 16.8	4.5 5.0	-- --	3.25 4.00	0.25 0.75	0.75 max	0.050 max	0.025 max	0.025 max	-- --	-- --

TABLE III. CALCULATED ELASTIC CRACK-MOUTH-OPENING DISPLACEMENT, v , AND LOAD-LINE DISPLACEMENT, d , FOR A THREE-POINT BEND SPECIMEN

a/w	vEB/P	dEB/P
0.00	0.00	19.09
0.20	7.07	23.58
0.40	20.83	39.01
0.60	64.36	88.28
0.80	323.9	365.0
0.95	6026.0	6147.0

TABLE IV. J_{Ic} RESULTS FOR STAINLESS STEEL PLATE
AND WELD-METAL IN VARIOUS CONDITIONS

Specimen Number	Condition	J-Integral Toughness; J_{Ic} KN/m	Effective Yield; S_y MPa	Validity Ratio; $BS_y/25J$
95-15 Plate; L-T:				
AP-L1	treat, age (ref 3)	185	1000	1.30
AP-L2		173		1.39
DP-L1	treat, age	198	943	0.51
DP-L2		183		0.56
95-15 Plate; T-L:				
AP-T1	treat, age (ref 3)	47	1010	5.16
AP-T2		44		5.51
DP-T1	treat, age	66	998	1.63
DP-T2		70		1.54
15-5 PH Plate; T-L:				
15-T1	treat, age	192	1100	1.09
15-T2		238		0.88
95-14 Weld:				
UW-1	weld, treat, age	94	1230	1.33
UW-2		79		1.57
15-500 Weld:				
5-3	as welded	124	1050	0.92
5-4		107		1.07
5A-1	weld, age	76	1220	2.05
5A-2		156		1.00
5S-3	weld, treat, age	157	1200	0.82
5S-4		157		0.82
17-400 Weld:				
7-1	as welded	103	1280	1.40
7-3		105		1.38
7A-3	weld, age	147	1280	1.04
7A-4		76		2.03
7S-1	weld, treat, age	167	1140	0.84
7S-2		135		1.04

TABLE V. CALCULATED STRESS INTENSITY FACTOR, K, FOR STANDARD SINGLE-EDGE CRACK SPECIMEN AND DOUBLE-EDGE CRACK WELD SPECIMEN LOADED IN THREE-POINT BENDING

a/W	[KBW ^{3/2} /PS] Standard; S/W = 4; One Crack	[KBW ^{3/2} /PS] Weld; S/W = 11; Two Cracks
0.098	0.84	0.93
0.196	1.16	1.28
0.295	1.50	1.64
0.393	1.94	2.11
0.491	2.59	2.81
0.589	3.62	3.94
0.688	5.50	6.03
0.786	9.73	11.44

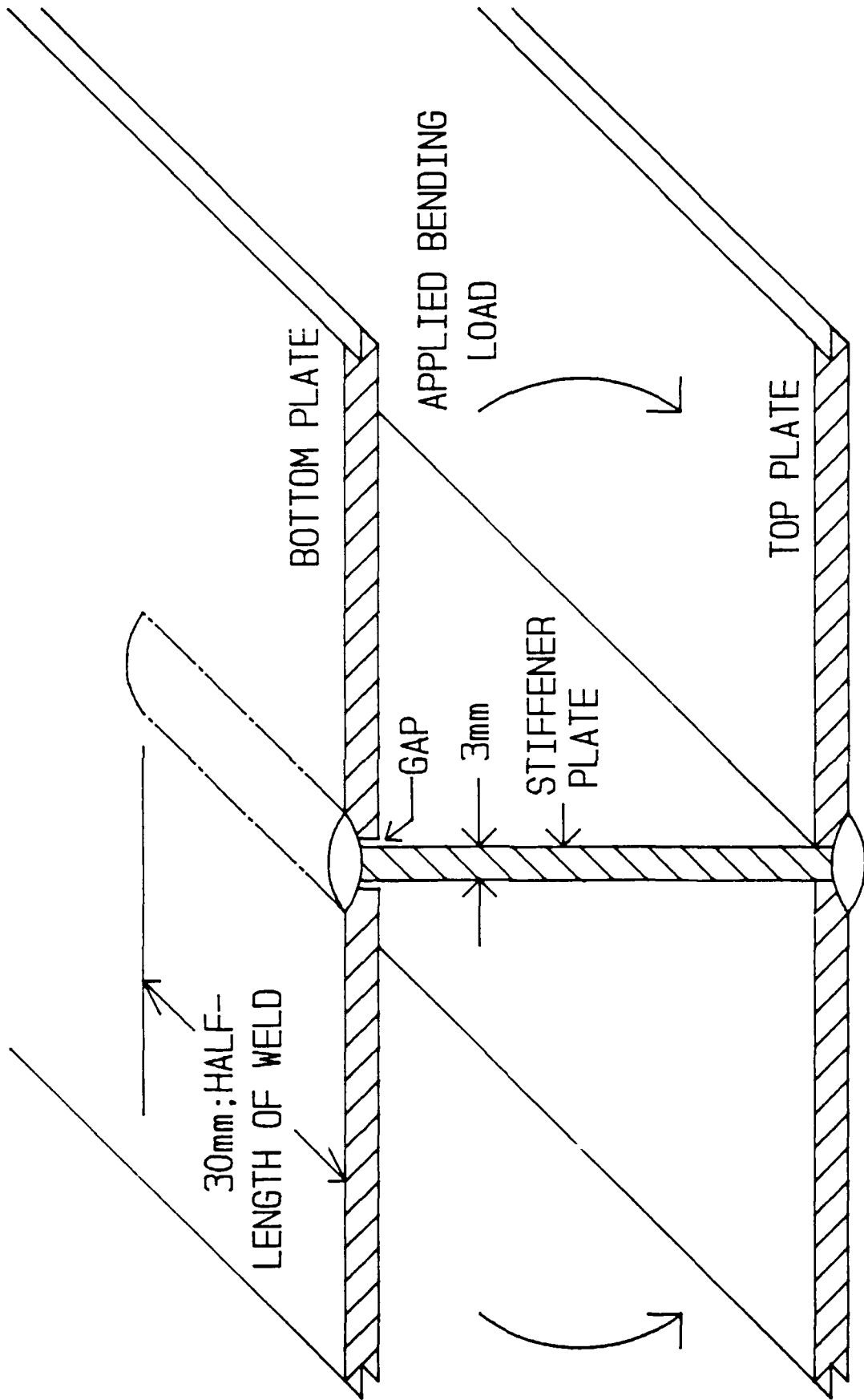


Figure 1. Welded box beam configuration showing orientation of test specimen.

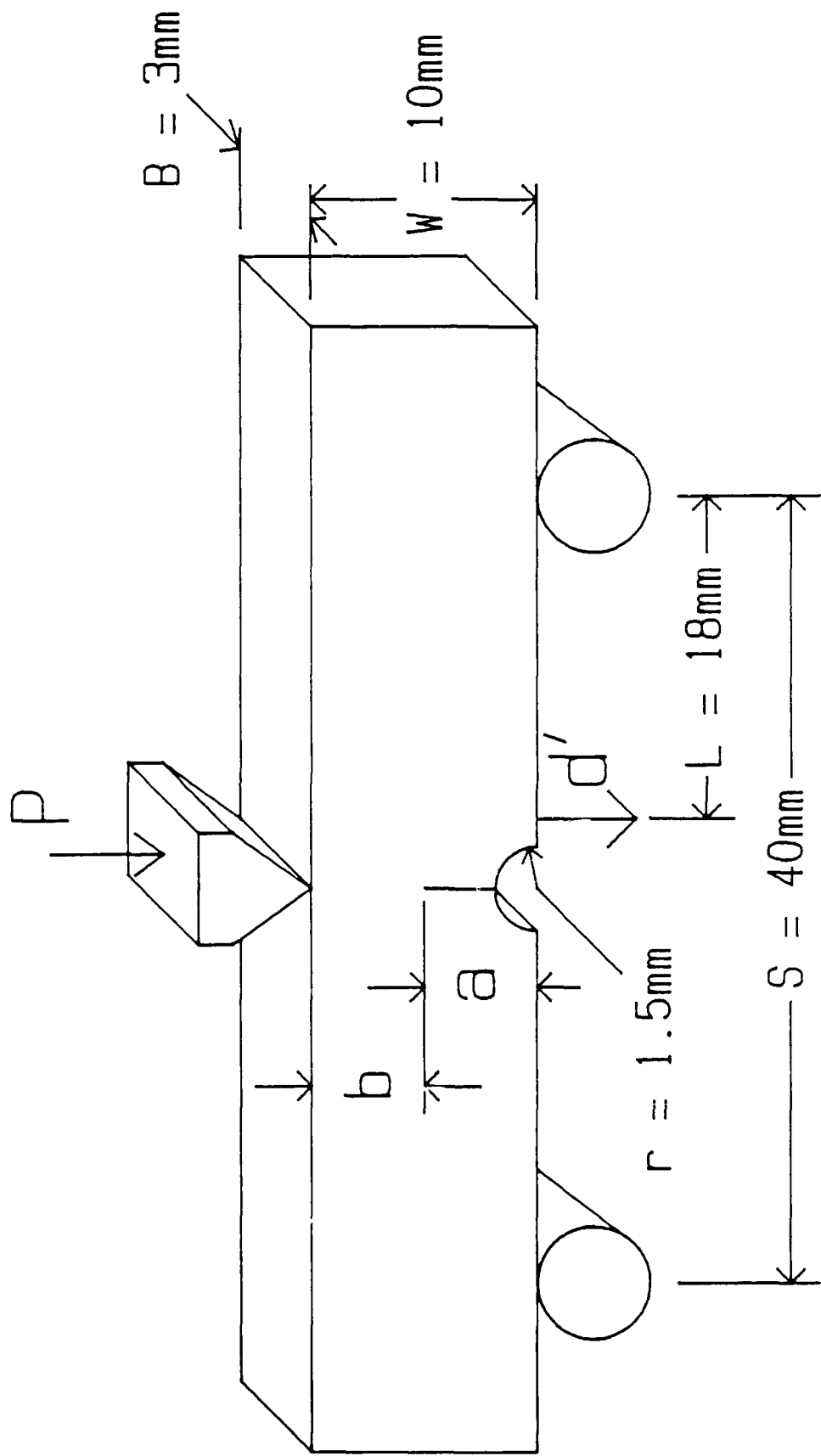


Figure 2. Test specimen for fracture toughness and fatigue crack initiation tests.

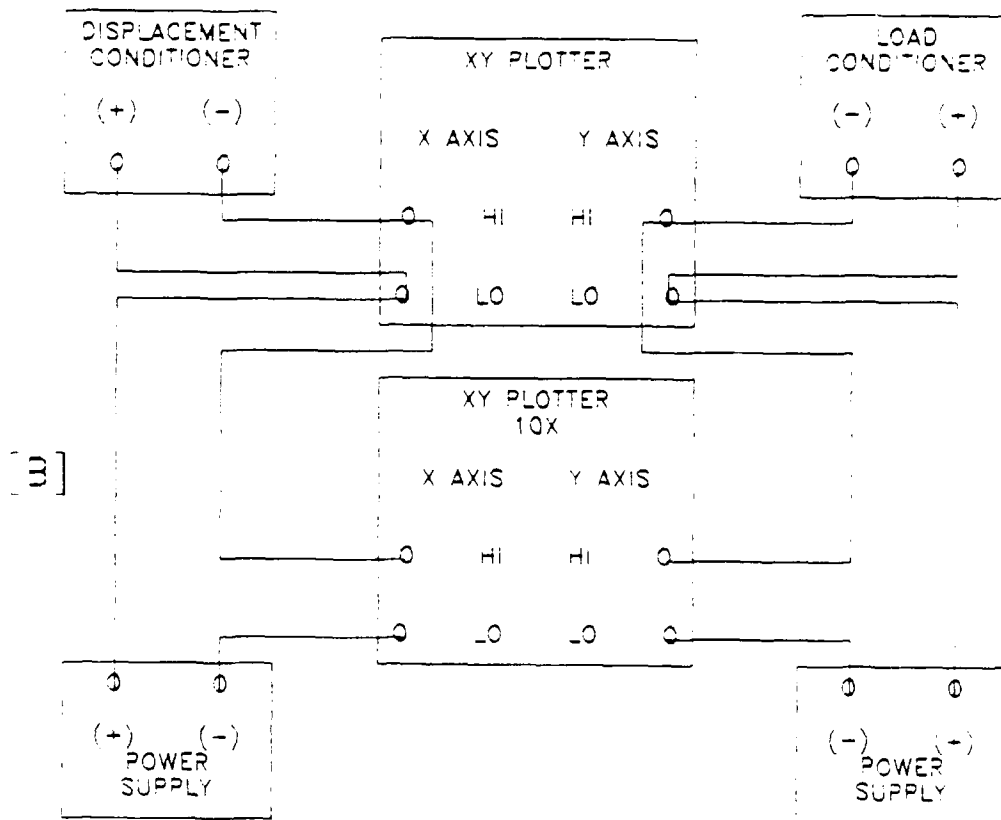
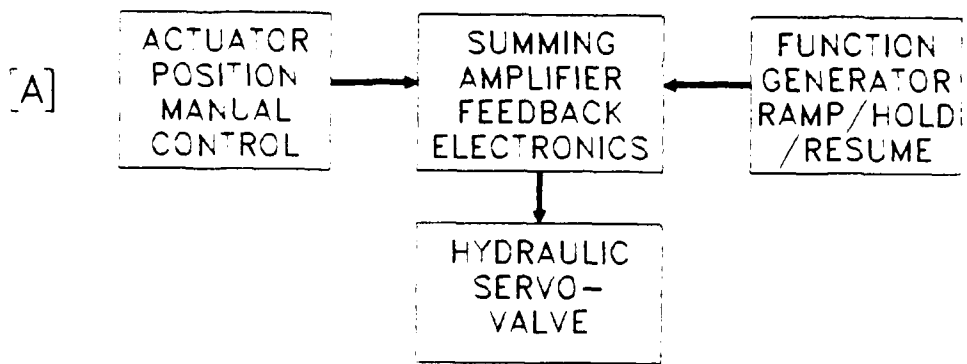


Figure 3. Test equipment for unloading-compliance J_{IC} tests.
 (a) Servo-hydraulic machine control
 (b) X-Y plotter arrangement

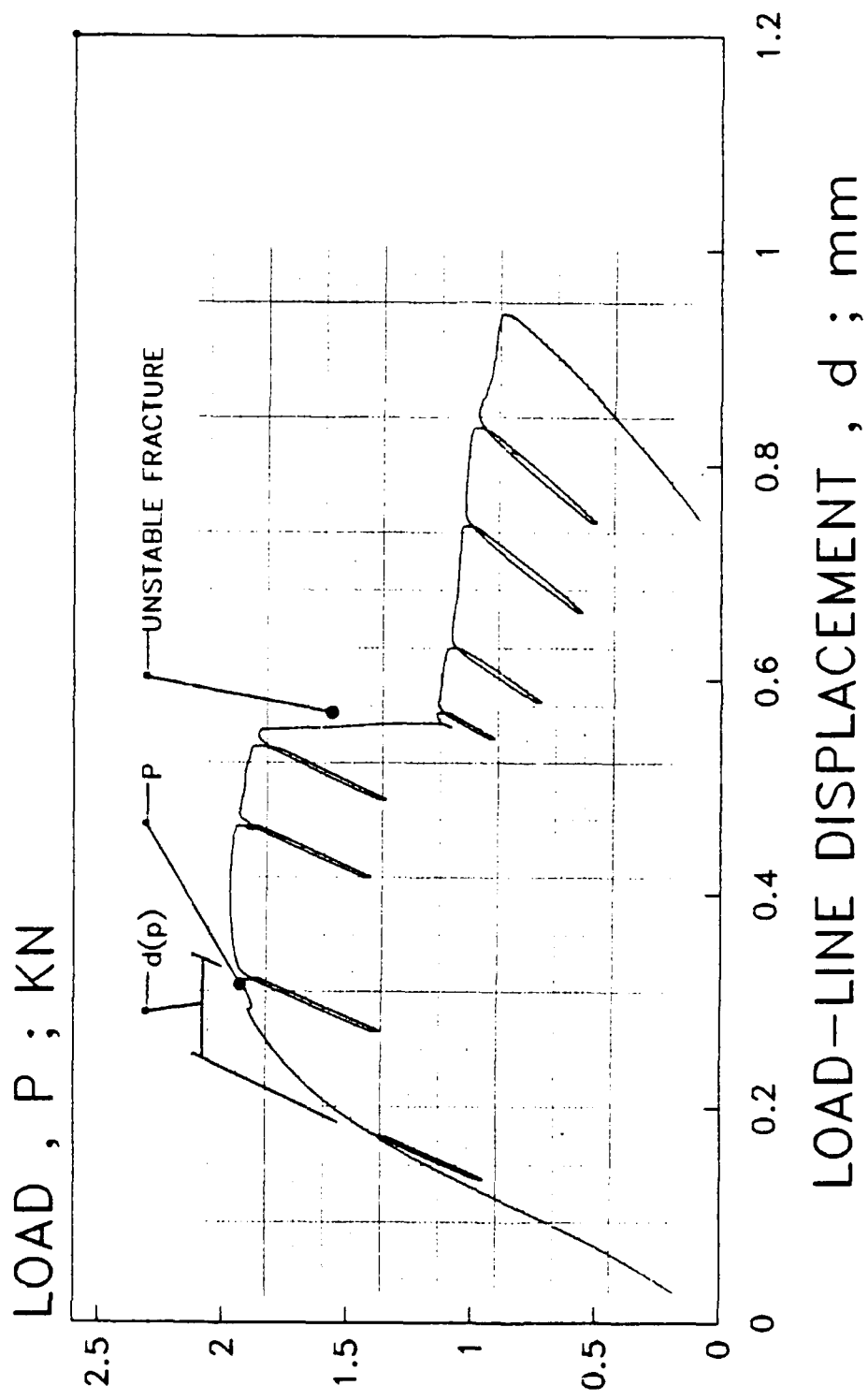


Figure 4. Load displacement behavior for 15-500 weld; welded and aged at 593°C.

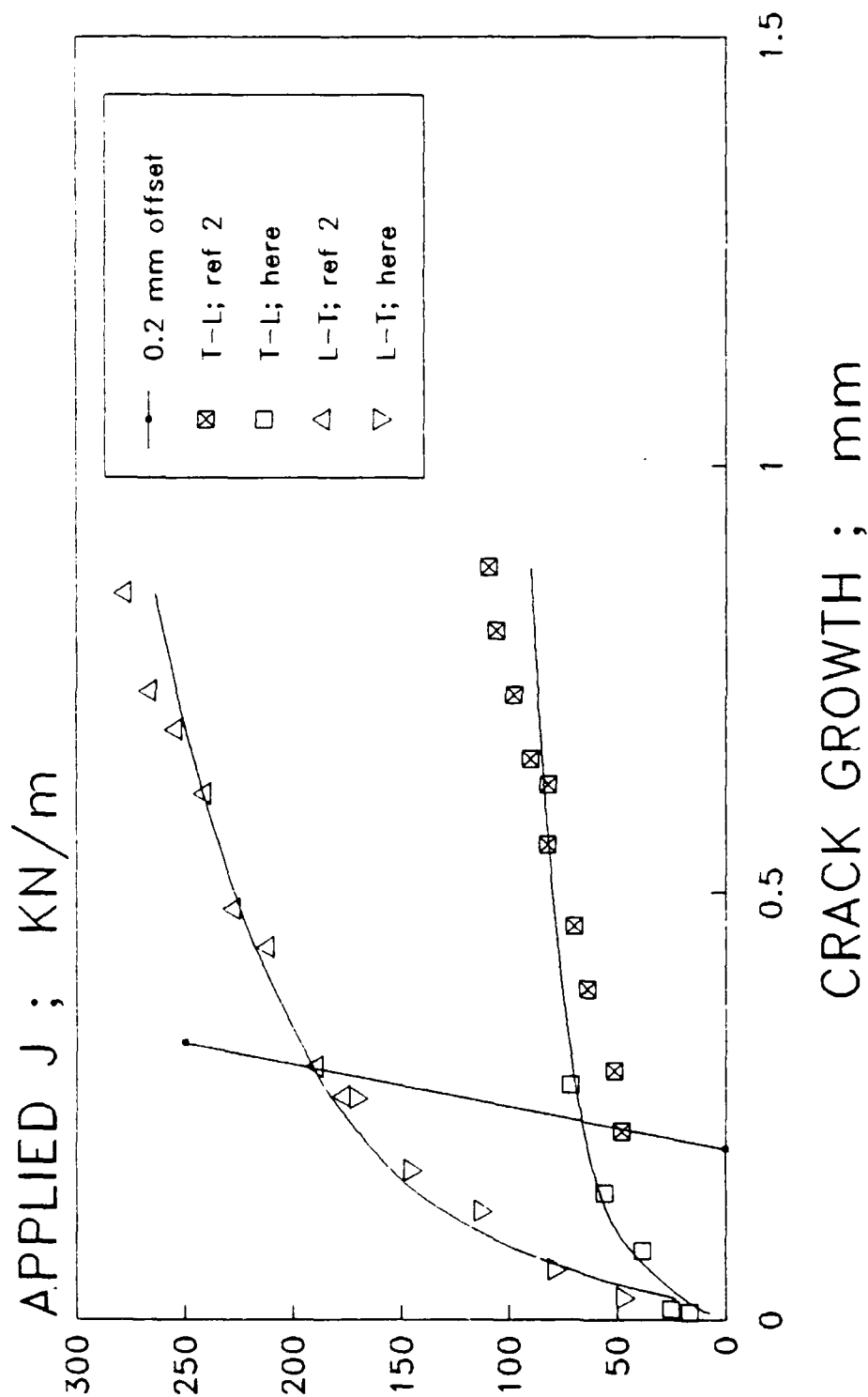


Figure 5. J versus crack growth for 95-15 plate; solution treated, aged at 530°C.
 #AP-T1; T-L orientation; ref 3
 #AP-L1; L-T orientation; ref 3
 #DP-T1; T-L orientation; current work
 #DP-L2; L-T orientation; current work

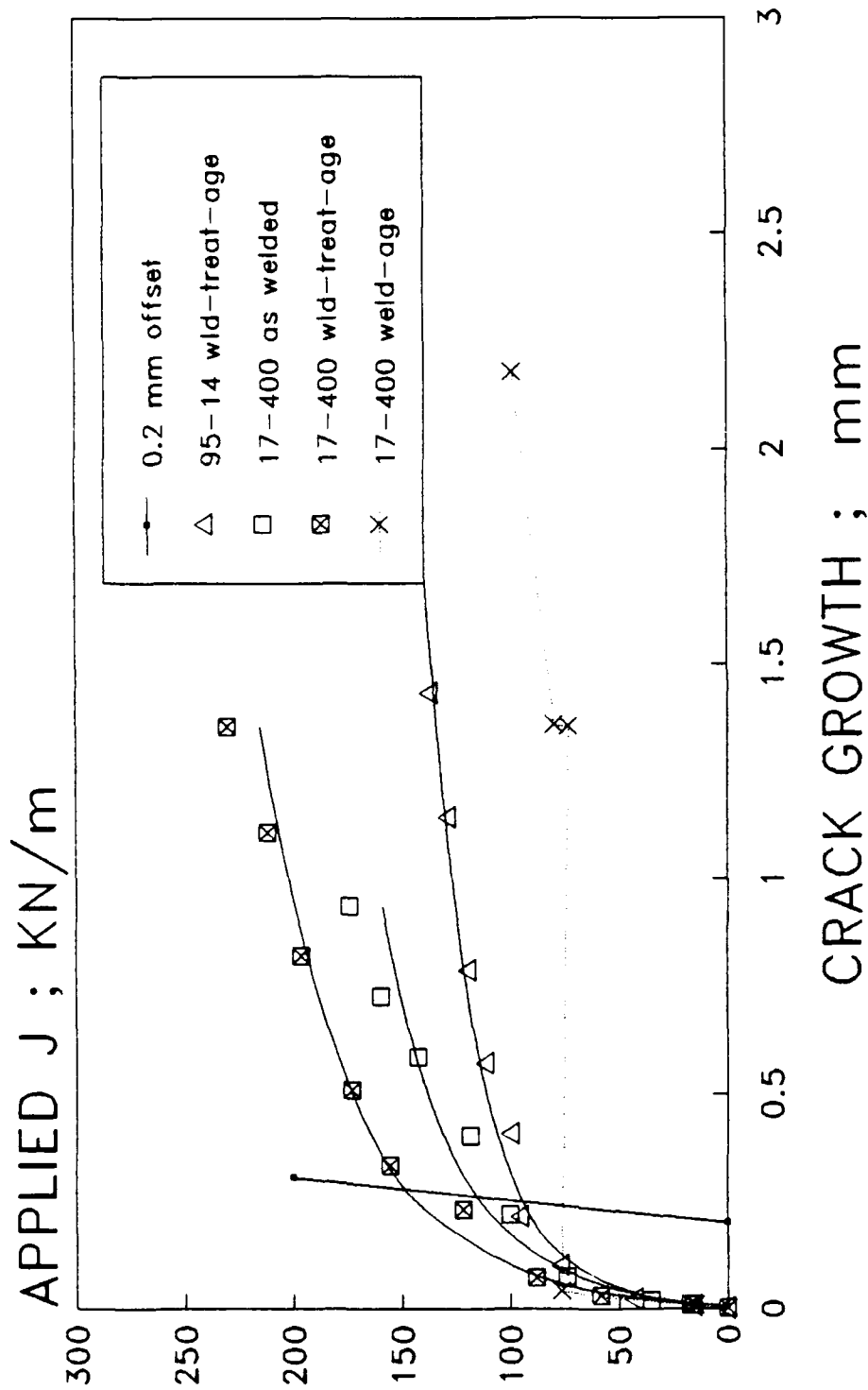
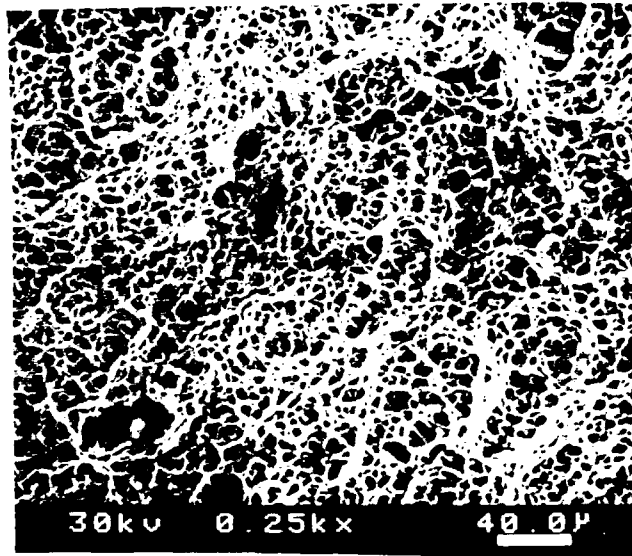
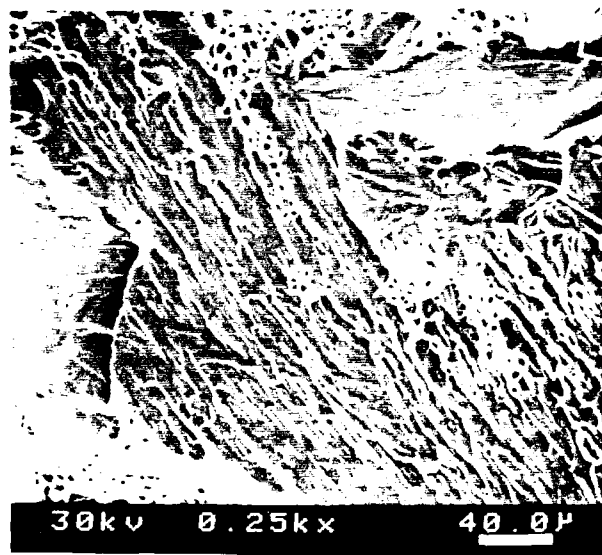


Figure 6. J versus crack growth for 17-400 and 95-14 welds in various conditions.
 #DW-1; 95-14, welded, treated, aged at 530°C
 #7-1; 17-400, as-welded
 #7A-4; 17-400, welded, aged at 593°C
 #7S-2; 17-400, welded, treated, aged at 593°C



(a) welded, treated, aged



(b) welded, aged

Figure 7. Scanning electron microscope fractographs of 17-400 welds.

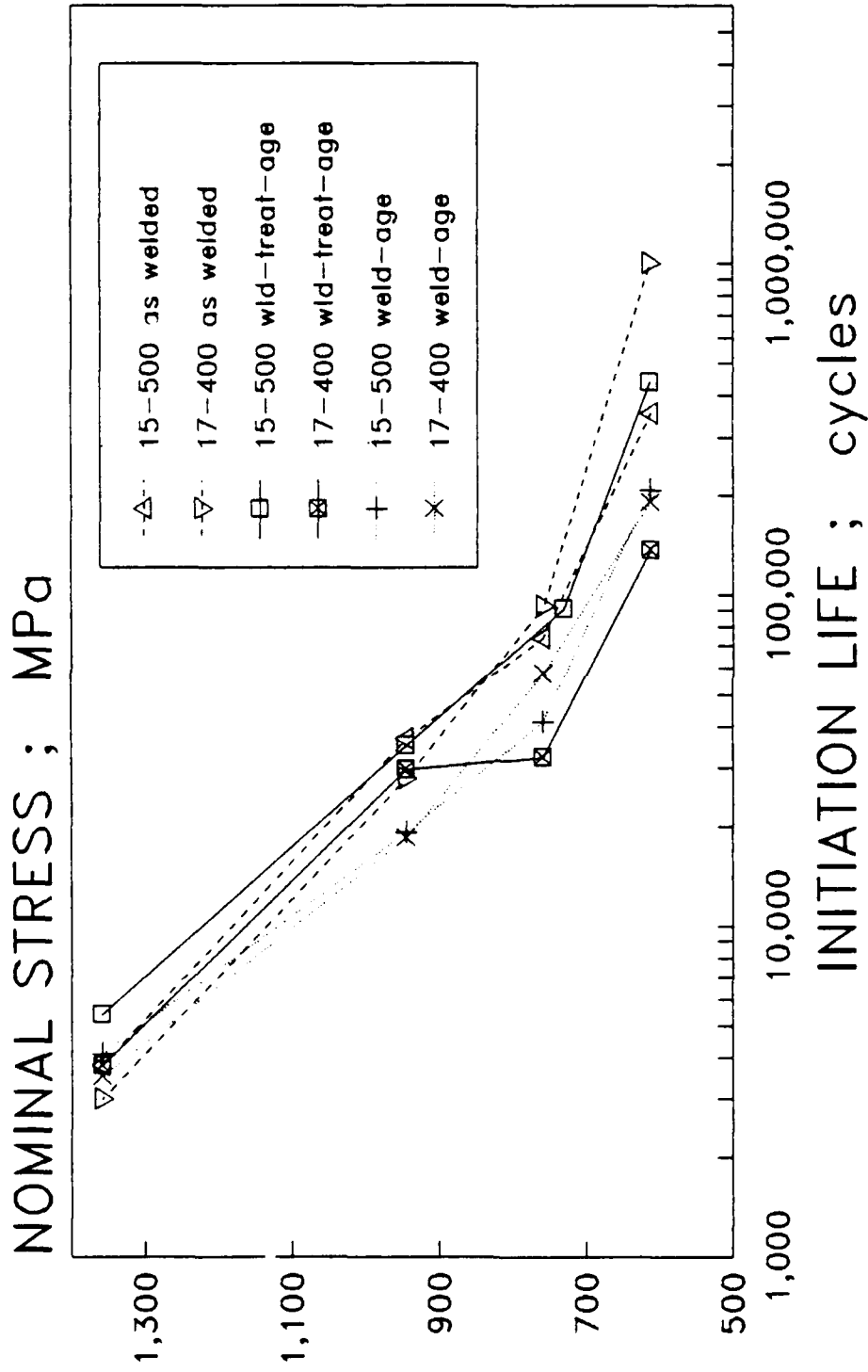


Figure 8. Fatigue crack initiation behavior of 15-500 and 17-400 welds in various conditions.

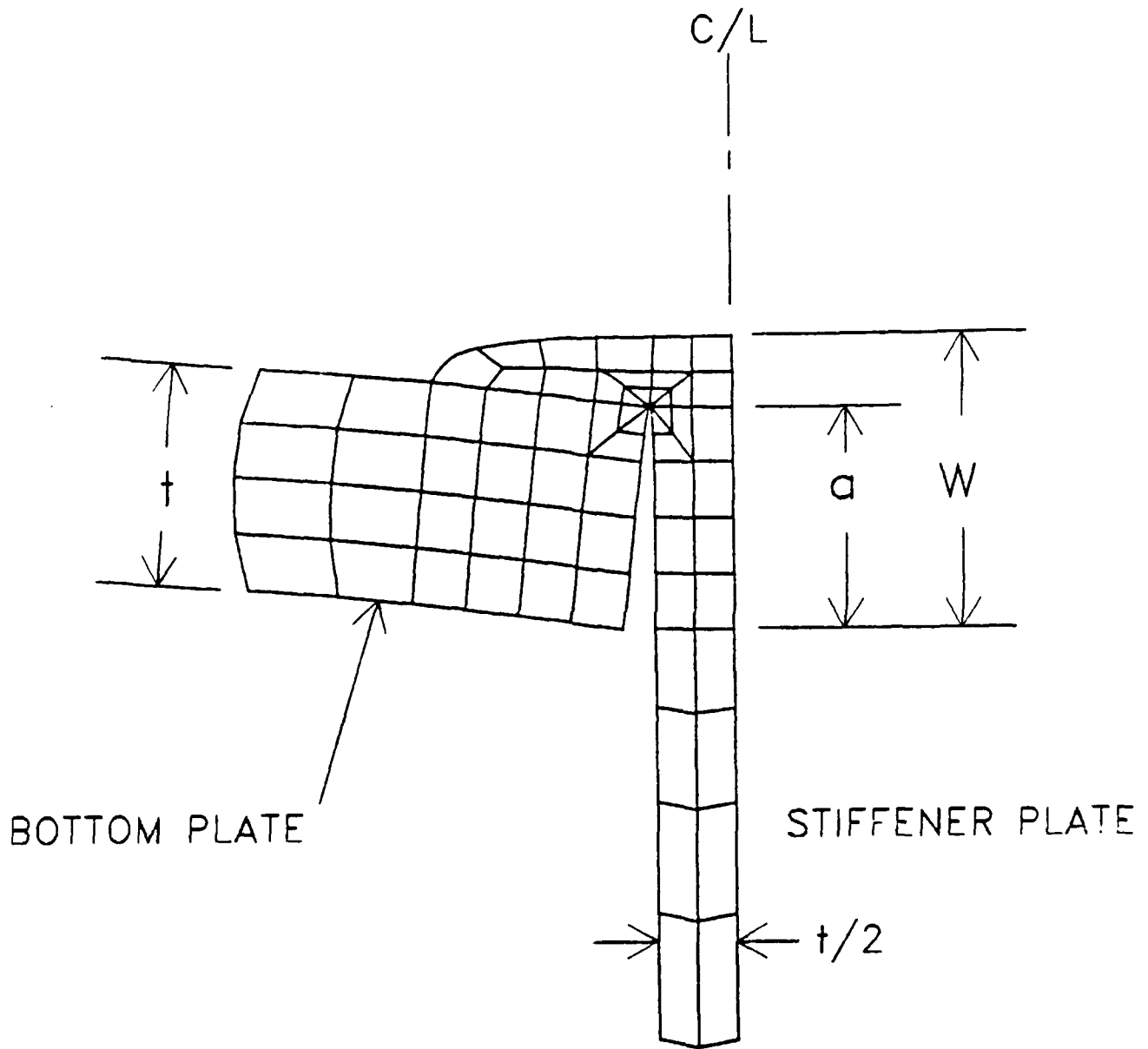


Figure 9. Deformed finite element model of stiffener-to-bottom plate weld specimen.

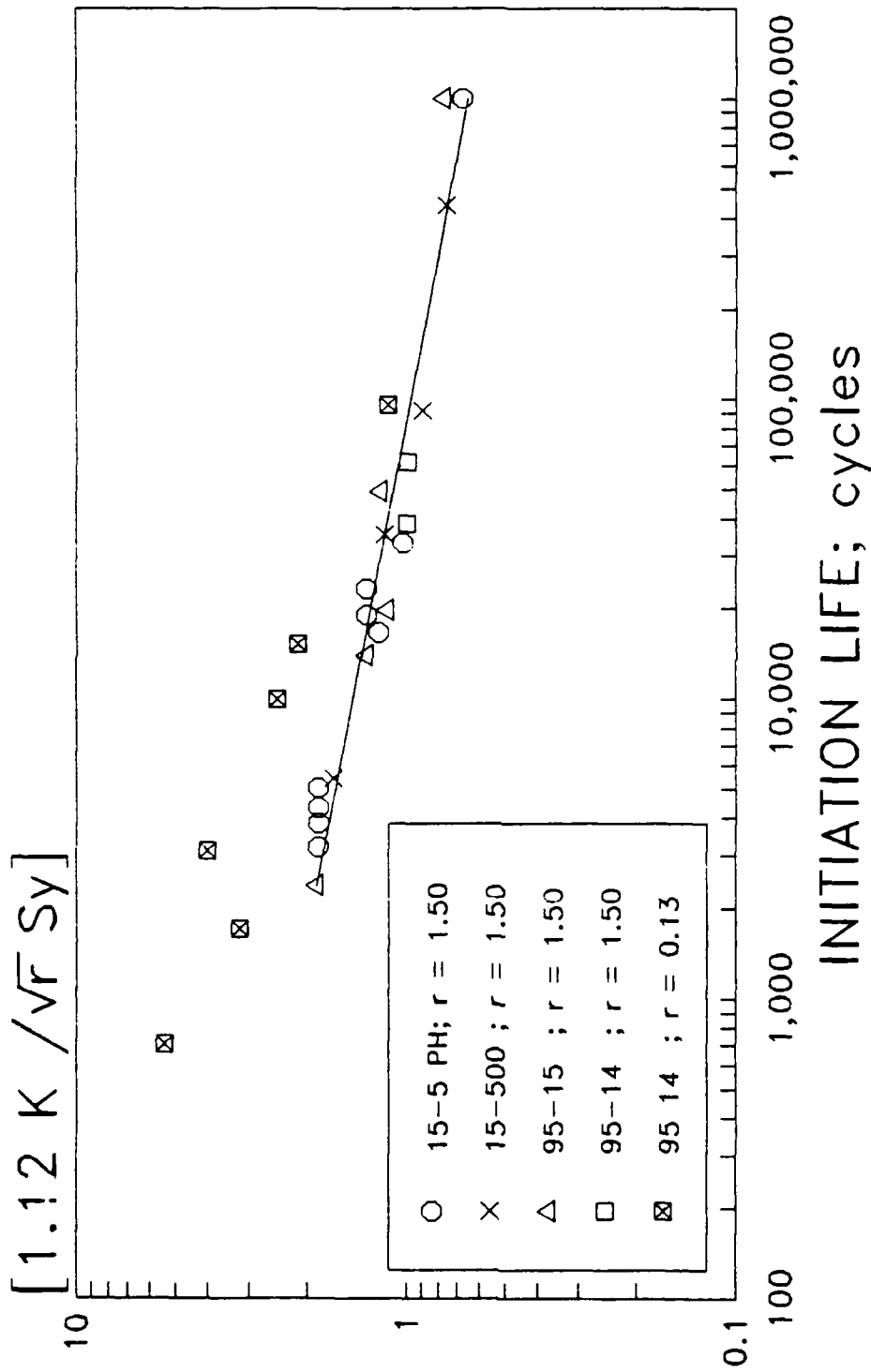


Figure 10. Fatigue life described by $[K/r^{1/2} S_y]$ parameter for specimens of different materials and configurations.

TECHNICAL REPORT INTERNAL DISTRIBUTION LIST

	<u>NO. OF COPIES</u>
CHIEF, DEVELOPMENT ENGINEERING DIVISION	
ATTN: SMCAR-CCB-D	1
-DA	1
-DC	1
-DM	1
-DP	1
-DR	1
-DS (SYSTEMS)	1
CHIEF, ENGINEERING SUPPORT DIVISION	
ATTN: SMCAR-CCB-S	1
-SE	1
CHIEF, RESEARCH DIVISION	
ATTN: SMCAR-CCB-R	2
-RA	1
-RM	1
-RP	1
-RT	1
TECHNICAL LIBRARY	
ATTN: SMCAR-CCB-TL	5
TECHNICAL PUBLICATIONS & EDITING SECTION	
ATTN: SMCAR-CCB-TL	3
DIRECTOR, OPERATIONS DIRECTORATE	
ATTN: SMCWV-OD	1
DIRECTOR, PROCUREMENT DIRECTORATE	
ATTN: SMCWV-PP	1
DIRECTOR, PRODUCT ASSURANCE DIRECTORATE	
ATTN: SMCWV-QA	1

NOTE: PLEASE NOTIFY DIRECTOR, BENET LABORATORIES, ATTN: SMCAR-CCB-TL, OF ANY ADDRESS CHANGES.

TECHNICAL REPORT EXTERNAL DISTRIBUTION LIST

	<u>NO. OF COPIES</u>		<u>NO. OF COPIES</u>
ASST SEC OF THE ARMY RESEARCH AND DEVELOPMENT ATTN: DEPT FOR SCI AND TECH THE PENTAGON WASHINGTON, D.C. 20310-0103	1	COMMANDER ROCK ISLAND ARSENAL ATTN: SMCRI-ENM ROCK ISLAND, IL 61299-5000	1
ADMINISTRATOR DEFENSE TECHNICAL INFO CENTER ATTN: DTIC-FDAC CAMERON STATION ALEXANDRIA, VA 22304-6145	12	DIRECTOR US ARMY INDUSTRIAL BASE ENGR ACTV ATTN: AMXIB-P ROCK ISLAND, IL 61299-7260	1
COMMANDER US ARMY ARDEC ATTN: SMCAR-AEE	1	COMMANDER US ARMY TANK-AUTMV R&D COMMAND ATTN: AMSTA-DDL (TECH LIB) WARREN, MI 48397-5000	1
SMCAR-AES, BLDG. 321	1	COMMANDER US MILITARY ACADEMY	1
SMCAR-AET-O, BLDG. 351N	1	ATTN: DEPARTMENT OF MECHANICS WEST POINT, NY 10996-1792	
SMCAR-CC	1		
SMCAR-CCP-A	1	US ARMY MISSILE COMMAND	
SMCAR-FSA	1	REDSTONE SCIENTIFIC INFO CTR	2
SMCAR-FSM-E	1	ATTN: DOCUMENTS SECT, BLDG. 4484 REDSTONE ARSENAL, AL 35898-5241	
SMCAR-FSS-D, BLDG. 94	1		
SMCAR-IMI-I (STINFO) BLDG. 59	2		
PICATINNY ARSENAL, NJ 07806-5000			
DIRECTOR US ARMY BALLISTIC RESEARCH LABORATORY ATTN: SLCBR-DD-T, BLDG. 305 ABERDEEN PROVING GROUND, MD 21005-5066	1	COMMANDER US ARMY FGN SCIENCE AND TECH CTR ATTN: DRXST-SD 220 7TH STREET, N.E. CHARLOTTESVILLE, VA 22901	1
DIRECTOR US ARMY MATERIEL SYSTEMS ANALYSIS ACTV ATTN: AMXSY-MP ABERDEEN PROVING GROUND, MD 21005-5071	1	COMMANDER US ARMY LABCOM MATERIALS TECHNOLOGY LAB ATTN: SLCMT-IML (TECH LIB) WATERTOWN, MA 02172-0001	2
COMMANDER HQ, AMCCOM ATTN: AMSMC-IMP-L ROCK ISLAND, IL 61299-6000	1		

NOTE: PLEASE NOTIFY COMMANDER, ARMAMENT RESEARCH, DEVELOPMENT, AND ENGINEERING CENTER, US ARMY AMCCOM, ATTN: BENET LABORATORIES, SMCAR-CCB-TL, WATERVLIET, NY 12189-4050, OF ANY ADDRESS CHANGES.

TECHNICAL REPORT EXTERNAL DISTRIBUTION LIST (CONT'D)

	<u>NO. OF COPIES</u>		<u>NO. OF COPIES</u>
COMMANDER US ARMY LABCOM, ISA ATTN: SLCIS-IM-TL 2800 POWDER MILL ROAD ADELPHI, MD 20783-1145	1	COMMANDER AIR FORCE ARMAMENT LABORATORY ATTN: AFATL/MN EGLIN AFB, FL 32542-5434	1
COMMANDER US ARMY RESEARCH OFFICE ATTN: CHIEF, IPO P.O. BOX 12211 RESEARCH TRIANGLE PARK, NC 27709-2211	1	COMMANDER AIR FORCE ARMAMENT LABORATORY ATTN: AFATL/MNF EGLIN AFB, FL 32542-5434	1
DIRECTOR US NAVAL RESEARCH LAB ATTN: MATERIALS SCI & TECH DIVISION CODE 26-27 (DOC LIB) WASHINGTON, D.C. 20375	1 1	METALS AND CERAMICS INFO CTR BATTELLE COLUMBUS DIVISION 505 KING AVENUE COLUMBUS, OH 43201-2693	1

NOTE: PLEASE NOTIFY COMMANDER, ARMAMENT RESEARCH, DEVELOPMENT, AND ENGINEERING CENTER, US ARMY AMCCOM, ATTN: BENET LABORATORIES, SMCAR-CCB-TL, WATERVLIET, NY 12189-4050, OF ANY ADDRESS CHANGES.